Origin of the Meissner Effect and Superconductivity

John P. Wallace

Casting Analysis Corp.,
8379 Ursa Lane, Weyers Cave,
Virginia 24486 USA

Michael J. Wallace

Freeport-McMoRan,
Phoenix, AZ 85050 USA

Superconductivity in most metals is due to the activity longitudinal spin waves binding electrons into pairs in such a way that the Meissner effect is generated along with the angular momentum responses in static magnetic fields. The bulk of these spin waves appear to be sourced by nuclear spins on the lattice. Experimentally longitudinal spin waves are not difficult to detect at room temperature as they form Bose-Einstein condensates that has onset temperatures for low mass entities well above room temperature. By forming these collective states allows them to be easily visible above noise.

CONTENTS

I. INTRODUCTION

Most metals possess active nuclear spins in addition to the spins of their conduction electrons. Only a few metals are devoid a nuclear spin population, see Table I and II. It is easy to experimentally monitor longitudinal spin waves at room temperature in iron due to a small population of active participating electronic spins because they efficiently form a coherent Bose-Einstein condensation with long lifetimes (Wallace, 2009a). These spin waves have a wide velocity range due to their small mass, unlike phonon that propagates at a single velocity. These properties make the longitudinal spin wave, $\mathbf{S}_{lsw}$ ideal for coupling with conduction electron spin, $\mathbf{S}_e$ via a $\mathbf{S}_{lsw} \bullet \mathbf{S}_e < 0$ allowing the interaction to form pairs that support superconductivity.

The recent announcements of near or above room temperature superconductivity in hydrogen rich alloys prompted a look of these spin rich alloys because of previous work where superconducting type activity was found above 77^oK in foils of aluminum and niobium contaminated with hydrogen (Wallace, 2011). The question arose: Could longitudinal nuclear spin waves mediate electron pairing and superconductivity while explaining the Meissner effect? The answer turns out to be yes. Longitudinal spin waves seem to be ubiquitous in most metals. They have some important properties including a small mass which gives them a range of velocities much greater than the speed of sound. A question as why these spin waves have been missing in action for so long has a simple answer, no one bothered to look for them.

Superconductivity is a completely non-classical phenomenon, poorly treated by modelers using a variation of quantum electrodynamics whose foundations are weak (Wallace and Wallace, 2023). Jorge Hisrch has logged a number of unanswered question about the inadequacy of the BCS model and later additions (Hirsch, 2009). The main complaint is about the inability of the modeler to explain the origin of Meissner effect. The phonon bonding hypothesis to create paired electrons is weak because longitudinal phonons operate at a fix velocity and possess no innate attractive potential, while electrons needing to be bound can be moving at considerably greater velocities. The BCS arguments also ignored the fact that T_c need not be isotope mass dependent via the phonon, as the band structure at low temperatures is extremely sensitive to isotope concentration ratios and the band structure plays a major role in fixing T_c.

II. A SIMPLE EXPERIMENT

To shows the existence of longitudinal spin waves requires only an induction source, a short coil, surrounding a long metal conductor. Very similar to the arrangement used in making eddy current measurements for properties or defects in the metal (Wallace, 2009a) (Wallace, 2011). However, instead of looking for the local eddy current response signal the detecting short coil is displaced away from the source to detect any propagating signals. The

Figure 1 ***Source and detector arrangement for generating and detecting the fields and exciton in a soft ferromagnetic iron alloy. The source is set near the end of the sample with a ground connection made to the bar close to the inductor to short circuit capacitive coupling to bar and coupling to the sensing inductor. This is important because the nuclear longitudinal spin waves produce a response about 1/100 that of what is found in annealed iron operating with conduction electrons.***

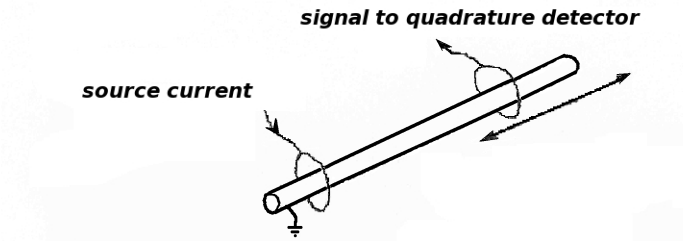

signal source and detector use was an SR865A lock-in-amplifier that allows an accurate measure of the amplitude and phase shift of a field created by its internal oscillator after traveling to a displaced detector coil, see Figure I. The instrument was operated over a frequency range of 10kHz to 4 MHz in this geometry testing a number of different non-ferromagnetic metals.

The electromagnetic analysis of the eddy current boundary value problem induces a local current that opposes the applied AC field. The geometry of the rod will seem to restrict any propagating field to have an axial symmetry. In practice what is detected away from the source propagating down the bar is a portion of a spherical wave front that rolls off as $\sim 1/r^3$. This is because the solid angle the detector captures goes as the *Sine* the angle formed by dividing the bars diameter to the displacement of the detector from the source. The energy pumped into the bar at the source ends up producing a spherical wave and not one constrained by the cylindrical geometry of the experiment. This spherically propagating field was generated by the eddy current itself because it contains the time dependence of this induced current and not the source field.

The geometry of this wave front being spherical is not a surprise as its a form generating the minimum dissipation due to not being able to generate eddy currents losses on its own. As this is an oscillating magnetic signal in time on a spherical wave front it is easy to show that $\nabla \times H = 0$. Therefore the wave front generates no induced currents from Ampere's Law $-\partial \mathbf{B}/\partial t = 0$. With no induced currents there are no eddy current losses. The detector simply records the response of the leakage field. A second test for the spherical wave front formation is to embed a source in a plate an on a circle centered on the source is to embed coils tangent to the circle around the source to monitor the roll off as a function of the angle from the normal to the source field. The fields only falls off 50% for a sensor perpendicular to the source at 90^o from the source and this is due to geometry of source interfering with the generated field. Unlike in free space doing this same test the field is not extinguished when the source and detector are oriented to 90^o to each other. As a check this experiment of coils embedded in a niobium plate both in line and perpendicular to source showed the characteristics of spherical wave front being generated.

When solving the electromagnetic boundary value problem for induced currents there is no solution predicting traveling longitudinal fields with spherical symmetry. The simple consultative relations used in Faraday-Maxwell equations 1 do not cover the quantum mechanical effects of how energy, especially in non-static modes is passed to the spins of the system (Pauli, 1973).

Table I **Some stable isotopes with nuclear magnetic moments for elements involved in superconductivity. The quantity P is used as a relative quality factor being the product of the % of isotopes in the metal with a nuclear magnetic moment's times the value of that magnetic moment.**

$P > 100$	$P < 100$	T_c K^o	Nuclear Mag. Moment %	Nuclear Moment	Moment × % = P
Nb		9.5	100	6.13	613
Tc		7.77	100	5.66	566
	Pb	**7.19**	**22**	.58	12.7
V		5.38	100	5.14	514
Ta		4.48	100	2.34	234
	Hg	4.15	30	-.55, +.50	15
In		3.4	100	5.51	551
	Sn	**3.7**	**16**	1.04	16
Tl		2.39	100	1.62	162
Re		1.4	100	3.17	317
Al		1.14	100	3.64	364
Ga		1.09	100	∼2.2	220
	Mo	.92	24	± .91	22
	Zn	**.875**	**4**	.87	3.5
	Os	.65	18	.65	11.7
	Cd	.56	12	.21	2.5
	Zr	.54	11	-1.3	14
	Ru	.51	29	-.69,-.28	15
	Ir	.14	100	.16	16
	Hf	.12	32	.655	21
	W	.012	14	.12	1.7

Table II **Some stable isotopes with nuclear magnetic moments for elements involved in alloys that are superconducting. This table raises the question if there exist longitudinal spin waves using the nuclear moments that are active. Then there is the complication of localized electronic spins supporting longitudinal spin waves that could also give rise to electron pairing to support superconductivity.**

Elements in Compound SC	Nuclear Mag. Moment %	Nuclear Mag. Moment	Moment × % = P
Li	100	3.2	320
H	100	2.79	279
F	100	2.63	263
Cs	100	2.56	256
B	100	2.5	250
Cu	100	2.3	230
As	100	1.43	143
D	100	.86	86
N	100	.4	40
K	100	.39	39
Y	100	-.14	14

$$\mathbf{B} = \mu\mathbf{H}$$
$$\mathbf{J} = \sigma\mathbf{E} \qquad (1)$$

Metals with a fraction of their isotope possessing nuclear spins is more common than metals with no nuclear spins. However, the most common with a very small fraction of nuclear spins is iron where iron-57 is the only isotope possessing a nuclear spin in a concentration of 2.2%. This is fortunate since the electron spin concentration found in iron that are active in longitudinal spin waves can be compared to non-ferromagnetic metals where the nuclear spins should dominate the long range fields.

III. EXPERIMENTAL DETAILS

The experiment simply required recording the amplitude in nanovolts and the phase angle in degrees after manually displacing a snugly fitted coil from the source at different position on different metallic samples. While taking measurements usually at three different frequencies at each positions so that the first and second derivatives, $\partial\omega/\partial k$ and $\partial^2\omega/\partial k^2$ can be numerically computed. The sensor were made of 4 turns of #20 copper magnet wire with the detector having a series 50 ohm resistor. Very close to the source coil the bar was grounded to

Figure 2 $1/r^3$ **roll off in signal showing very little dissipation in an aluminum tube .0127 meters in diameter. This is the roll off expected for a spherical wave where the sensor has a finite sampling length along the bar. The $1/r^2$ roll off for a spherical wave is modified by the finite sampling length of the coil that goes as the $sin(\theta)$ where θ is the angle of from the center of the source coil to the middle of the detector coil on the outside diameter of the sample. This produces the additional factor of $1/r$. The weak attenuation is feature of a uniform wave front that induces no local currents.**

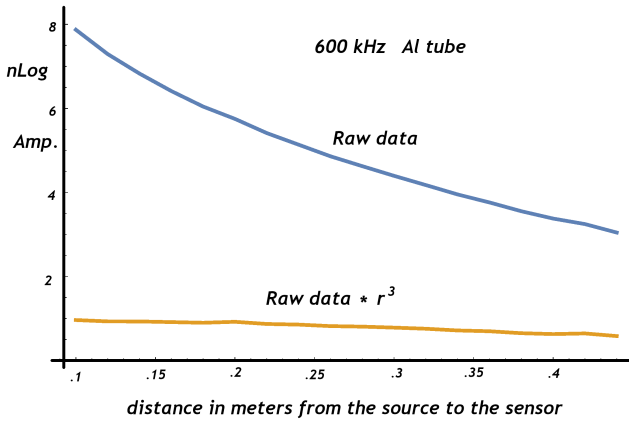

short circuit capacitive coupling between the coil and the bar. The source was driven at an amplitude of 2 volts which translates to a current range about 50 milliamps producing a field of $\sim 10^{-6}$ Tesla at the center of coil with a diameter of .127 meters. Phase calibration is done with the source and detector coils empty but in the same orientation as the test. Those phase offsets are due to the circuitry and wiring and need to be subtracted from the measured data on a sample. The gross absolute phase offsets are due to the eddy current generated in the sample and for those to calculated a very well characterized sample is need. Those phase angles are not essential in these measurements as they will be processed out by differences.

These drives were at a much lower level compared to the earlier work in iron where the drive level supported three simultaneous frequency just below an operating point where there was no non-linear behavior. The response in iron is nearly two orders of magnitude greater with the same drive levels. Non-linear meaning where product states of the type $\omega_1 \pm \omega_2$ and $\omega_1 \pm 2\omega_2$ were produced. The consideration here is that what is being measured are not single exciton properties but that of a Bose-Einstein condensate that is made of a collection of coherent components. Because of the low mass of the spin waves the BEC onset temperature is well above room temperature (Wallace, 2009a). In both the ferrous and non-ferrous metals a strong transverse magnetic field of greater than .1 $Tesla$ produces no effect on the spin

wave propagation to the limits of the the measurement. Whereas, the accuracy of the amplitude measurements can be made to within 1 or 2 nano volts the phase angle measurements are not as accurate because of the accumulated errors of the two quadrature channels especially at distances greater than .3 meters. At .1 meters and under it is possible to measure the absolute phase angles to $.01^o$ degrees of arc.

IV. MASSES AND VELOCITIES

The complete relativistic wave equation (Wallace and Wallace, 2023) in the laboratory frame will be used for the longitudinal spin wave. Neither the Schrödinger, Dirac, nor the Klein-Gordon equation are of use as the all fail to handle both energy conservation and relativity properly.

$$\frac{\hbar^2}{2m}\{\nabla^2\phi - \frac{1}{c^2}\frac{\partial^2\phi}{\partial t^2}\} + i\hbar\frac{\partial\phi}{\partial t} = (V + \frac{V^2}{2mc^2})\phi \quad (2)$$

With the potential being zero, $V = 0$, the equation reduces to:

$$\frac{\hbar^2}{2m}\{\nabla^2\phi - \frac{1}{c^2}\frac{\partial^2\phi}{\partial t^2}\} + \frac{2im}{\hbar}\frac{\partial\phi}{\partial t} = 0 \quad (3)$$

taking the trial solution for a spherical wave a:

$$\phi(r) = A\frac{e^{i(\kappa r - \omega t)}}{r} \quad (4)$$

This yields the dispersion relation on substituting equation 4 into 3:

$$\begin{aligned} \omega^2 - \frac{2mc^2}{\hbar}\omega + c^2\kappa^2 = 0 \\ E = \hbar\omega = mc^2\{1 - \sqrt{1 - \frac{\hbar^2\kappa^2}{m^2c^2}}\} \end{aligned} \quad (5)$$

From the raw phase shift data at a fixed displacement along the bar or plate as function of frequency it is possible to estimate the spin wave velocity and its mass by taking the first and second derivatives. The propagation vector, κ, is determined by the measured phase shift of the field, θ as as function of displacement, r.

$$\kappa(\omega) = \frac{\theta(\omega)}{r} \quad (6)$$

Both r and θ can be measured so that k can be computed. Numerically both the first and second derivative of $\omega(\kappa)$ as a function can be estimate when $\omega_2 - \omega_1 = \omega_1 - \omega_0 = \Delta\omega$. In order to compute the velocity and mass of the longitudinal spin waves two numerical derivatives are required

Figure 3 **The relativistic dispersion curve from equation 5 is compared to the non-relativistic form $E = \hbar^2\kappa^2/2m$ that is a simple parabola. If a relativistic correction is attempted by adding a factor of γ to the non-relativistic dispersion relation the computed velocities approach the speed of light which is not realistic.**

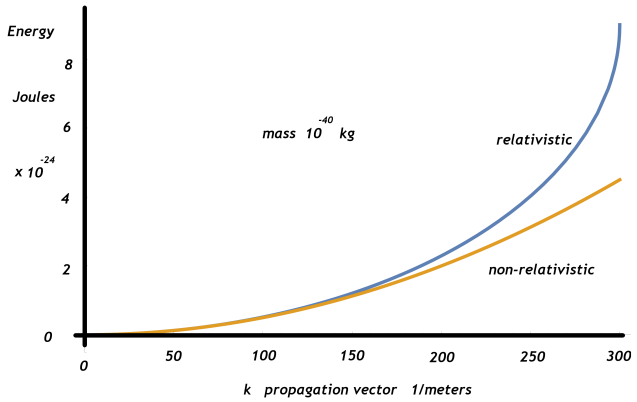

$$\begin{aligned} \frac{\Delta\omega}{\Delta\kappa} &= \frac{r\Delta\omega}{\theta_1 - \theta_0} \\ \frac{\Delta^2\omega}{\Delta\kappa^2} &= 2\Delta\omega\frac{2\theta_1 - \theta_2 - \theta_0}{(\theta_2 - \theta_0)(\theta_2 - \theta_1)(\theta_1 - \theta_0)}r^2 \end{aligned} \quad (7)$$

Taking the derivative of ω with respect to the propagation vector, κ, in equation 5 is the first step.

$$\frac{\partial\omega}{\partial\kappa} = \frac{v}{\sqrt{1 - \frac{v^2}{c^2}}} \quad (8)$$

$$v = \frac{\partial\omega}{\partial\kappa}\frac{1}{\sqrt{1 + \frac{\frac{\partial\omega}{\partial\kappa}^2}{c^2}}} = \frac{\Delta\omega}{\Delta\kappa}\frac{1}{\sqrt{1 + \frac{\frac{\Delta\omega}{\Delta\kappa}^2}{c^2}}} \quad (9)$$

In order to extract the mass, m, a relation using the second derivative of equation 5 of ω with respect to the propagation vector is required, where $\gamma = 1/\sqrt{1 - v^2/c^2}$.

$$\frac{\partial\omega}{\partial\kappa} = \frac{\hbar}{m}\frac{\kappa}{\sqrt{1 - \frac{\hbar^2\kappa^2}{m^2c^2}}} \quad (10)$$

$$\frac{\partial^2\omega}{\partial\kappa^2} = \frac{\hbar}{m}\gamma + \frac{\hbar}{m}\frac{v^2}{c^2}\gamma^3 \quad (11)$$

$$m = \frac{\hbar}{\frac{\Delta^2\omega}{\Delta\kappa^2}}\{\gamma + \frac{v^2}{c^2}\gamma^3\} \quad (12)$$

Now the velocity and the mass can be computed from the data derived first and second derivatives of ω with respect to propagation vector. These are not single particle velocities rather the velocity and mass of Bose-Einstein condensations.

Figure 4 ***Longitudinal spin wave's spherical propagating wave front is a large scale structure with a long wavelength on the order of a meter compared to scale required to bind electrons. A single spin wave had the capacity to bind opposite momentum electrons to produce a zero momentum state for the bound pair. The pair can can then interact with an external field so long as the field does have the strength to break the magnetic bond between the propagating spherical wave front of the longitudinal spin wave and the electron's spin. What is required of the spin wave is a velocity that matches the electrons' velocities. Because the longitudinal spin waves possessing mass have a range of velocities from zero upwards unlike the phonon that only operates at the speed of sound.***

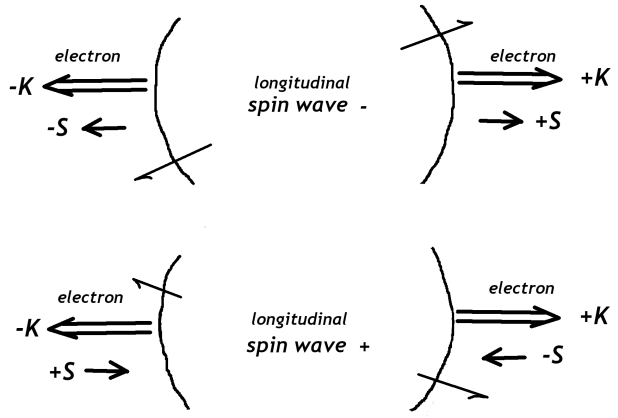

V. SUPERCONDUCTIVITY

Shielding the behavior the electrons that participate in forming pairs to act as a boson is probably an essential feature for a metal to become superconducting. Hirsch noted only hole conductors have superconducting properties. He was concerned about charge imbalances going through the superconducting transition. The imbalances would be caused the effect of the surface on particle motion. Only a more agile charge carrier could screen the

Table III **The Fe samples were taken at 80-120-160 kHz all the others were taken at .5-1.0-1.5 MHz. Al, Cu, Ti64, and Fe rods were .127 m in diameter except for the W rod that was .0095 m in diameter. The pure Nb and Ti samples ($< 99.9999\%$ *metal purity* however these bars probably contain a significant amount of hydrogen) had rectangular cross sections of .0034 x .0112 m and .0051 x .0117 m respectively. The copper sample was annealed oxygen free high conductivity. The iron was 99.9% metal content and the aluminum and Ti64 were commercial grade. The data was processed by the numerical derivatives from equation 7 used for velocity and mass in equations 9 and 12. A pair of velocities were computed from the two pair of frequency ranges.**

metal	**source to detector** *meters*	**Velocity range** m/sec	**Mass** **kg**	**Amp.** μV $\sim .1m$
Fe	.1	$3.7 - 5.0\ 10^5$	$9.6\ 10^{-36}$	75
Nb	.06	$2.7 - 12.3\ 10^6$	$1.6\ 10^{-37}$	
Nb	.09	$2.2 - 2.7\ 10^6$	$6.2\ 10^{-36}$	1.3
Al	.1	$1\ 10^7$	$8.7\ 10^{-37}$	2.9
Al	.15	$1.6 - 2.1\ 10^7$	$7.2\ 10^{-38}$	
Al	.20	$2.3 - 5.0\ 10^7$	$8.2\ 10^{-39}$	
Ti64	.1	$3.3 - 4.3\ 10^6$	$1.9\ 10^{-36}$	3.3
Ti64	.15	$5.3 - 6.5\ 10^6$	$1.5\ 10^{-36}$	
Ti64	.2	$7.5 - 1.5\ 10^6$	$9\ 10^{-38}$	
Ti	.06	$1.7 - 4.2\ 10^6$	$1.1\ 10^{-36}$	3.2
Ti	.09	$3.5 - 6.2\ 10^6$	$2.6\ 10^{-37}$	
Zn	.1	$.67 - 1.2\ 10^7$	$1.6\ 10^{-39}$	2.4
Zn	.15	$1.2 - 2.0\ 10^7$	$5.8\ 10^{-38}$	
Zn	.2	$2.1 - 4.7\ 10^7$	$9.6\ 10^{-39}$	
W	.12	$7.6 - 17.2\ 10^6$	$6.8\ 10^{-38}$	~ 2
Cu	.1	$1.0 - 1.5\ 10^7$	$1.3\ 10^{-39}$	3.1
Cu	.15	$1.6 - 2.6\ 10^7$	$3.6\ 10^{-38}$	
Cu	.2	$2.3 - 5.5\ 10^7$	$7.1\ 10^{-39}$	

superconducting interior. Any long range electrostatic field at that point would inhibit the transition to superconductivity. The facility of having a spin free screening agent, holes, more agile than the electrons being in the superconducting state is a major feature of the entire process.

Figure 5 **In order to achieve the Messiner effect there are three very important details. First you need a longitudinal spin wave to couple to two electrons via their spins which are aligned along their directions of motions. The second is those two electrons have opposite k, propagation vectors. Third there is a magnetic field present which the electrons will be forced to rotate around without breaking their connection to the longitudinal spin wave. This rotation about the field will cause the imposed external field to be canceled. The electrons will now have an axial angular momentum and for momentum to be conserved the solid they are in will rotate in the opposite direction.**

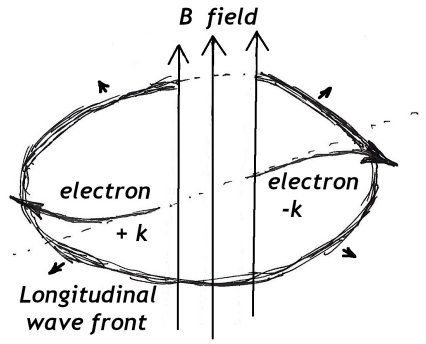

VI. INERTIA OF A LONGITUDINAL SPIN WAVE

The principal inertia the spin wave must over come is the inertia due to rotating its magnetic moment. In iron the inertia of a free electron is about two orders of magnitude greater than that for the nuclear spins. This correlates to the velocity difference between the two groups. The interesting entity is the proton that is extremely supple and may contribute to its alloying efficiency in superconductors.

ACKNOWLEDGMENTS

Sampath Purushothaman who brought up the matter of hydrogen alloyed metallic high temperature superconductors.

REFERENCES

Table IV **Moment of inertia estimated using the charge radius and the mass in the relation $mr^2/2$. For the free electron the electrostatic charge radius was used (Wallace and Wallace, 2015). For the nucleons the relation $1.25 \times A^{1/3} fm$ was used where A is the mass number. The free electron behavior might be reflected in the spin wave behavior in iron. Where the other non-ferrous metals have a reduced over rotational inertia.**

isotope	**mass kg** $\times 10^{-27}$	**radius meters** $\times 10^{-15}$	**I** $\times 10^{-60}$ $m\ kg^2$	**I** $\times\ \mu$
bound ele.	.00091	$\sim 1\ 10^5$	$4.55\ 10^{-51}$	$4.22\ 10^{-74}$
free ele.	.00091	$7.72\ 10^2$	$2.71\ 10^{-55}$	$2.52\ 10^{-78}$
^{201}Hg	336.378	7.18	$8.67\ 10^{-54}$	$2.42\ 10^{-80}$
^{199}Hg	333.027	7.18	$8.58\ 10^{-54}$	$2.16\ 10^{-80}$
^{93}Nb	155.5038	5.578	$2.42\ 10^{-54}$	$7.51\ 10^{-80}$
^{27}Al	45.160	3.71	$3.10\ 10^{-55}$	$5.7\ 10^{-81}$
proton	1.67262	.87	$6.33\ 10^{-60}$	$8.928\ 10^{-86}$

Faraday, M. (1832), Phil. Tan. R. Soc. Lond. **122**, 125.

Hirsch, J. E. (2009), "Bcs theory of superconductivity: the worlds largest madoff scheme?, arxiv 0901.4099,".

Pauli, W. (1973), *Pauli Lectues on physics volume 1 Electrodynamics* (MIT Press, Cambridge).

Wallace, J. (2009a), "Electrodynamics in iron and steel, arxiv:0901.1631v2 [physics.gen-ph],".

Wallace, J. (2009b), JOM **61** (6), 67.

Wallace, J. (2011), in *SSTIN10 AIP Conference Proceedings 1352*, edited by G. Myneni and et. al. (AIP, Melville, NY) pp. 205–312.

Wallace, J., and M. Wallace (2015), in *Science and Technology of Ingot Niobium for Superconducting Radio Frequency Applications*, Vol. 1687, edited by G. Myneni (AIP, Melville, NY) pp. 040004–1–14, *Electrostatics*.

Wallace, J., and M. Wallace (2017), *"yes Virginia, Quantum Mechanics can be Understood"* (Casting Analysis Corp., Weyers Cave, VA).

Wallace, J., and M. Wallace (2023), J. Phys. Astro. **11** (4), 337.

.